

Clustering and spin interactions in Fe-doped diamond

E M Benecha¹ and E B Lombardi¹

¹College of Graduate Studies, University of South Africa, P.O. Box 392, UNISA 0003, Pretoria, South Africa

E-mail: ebenecha@gmail.com

Abstract. The origin of high Curie temperature ferromagnetism in dilute magnetic semiconductors and oxides has often been attributed to clustering and crystallographic phase separation of magnetic atoms, which may have a detrimental impact on the properties of the host material for target applications. We present Density Functional Theory calculations on the stability and magnetic interactions of embedded Fe⁺¹ ions in diamond by considering various possible cluster configurations. We find that Fe ions have a strong tendency to form embedded clusters in diamond, with larger cluster sizes ($n > 3$) suppressing the induced spin moment. Also, we find that the electronic structure of the stable embedded Fe⁺¹ clusters is insulating, in contrast to homogeneous distribution, where a half metallic character with 100% spin polarisation at the Fermi level has been predicted. These results present important implications to the understanding of the properties of transition metal dopants in diamond, as well as in other dilute magnetic semiconductors where the effect of aggregation of dopants has generally been neglected.

1. Introduction

Ferromagnetic ordering of dopants in semiconductors continues to attract intense interest [1] for the development of a new generation of multifunctional devices capable of utilizing spin degrees of freedom in semiconductor materials [2, 3]. However, despite recent experimental successes on doping techniques and characterization of the ensuing properties of dopants in semiconductors, the origin and control of ferromagnetism in dilute magnetic semiconductor materials (DMSs) is not well understood [4]. Particularly, segregation and clustering effects of transition metal dopants (as opposed to homogeneous distribution) in semiconductors has been found to play an important role in determining the properties of the host material [4, 5].

Transition metal point defects in diamond have been a subject of significant research interest for many years since the discovery of optically and electrically active centers arising from use of transition metal solvent catalysts during high pressure-high temperature (HPHT) growth of synthetic diamond [6]. More recently, it has been demonstrated that defect centers in diamond, particularly the (N-V)⁻¹ center exhibits remarkable spin properties [7] suitable for quantum computing and optoelectronic applications.

Following the prediction by Dietl *et al* [8] that the Curie temperature of a DMS scales as the reciprocal of its lattice constant, there has been renewed interest in diamond aimed at finding suitable transition metal defect centers which may lead to room temperature ferromagnetic ordering due to diamond's small lattice constant (3.569 Å), compared to other semiconductors. In addition, diamond is a wide band gap semiconductor with attractive properties which makes it suitable for a wide range of electrical, electronic [6] and photonic [9] applications. So far,

substitutional Fe^{+1} [10] and divacancy Cr^{+2} [11] have been predicted to order ferromagnetically in diamond, while ferromagnetic ordering in Mn-doped diamond has been predicted to be unlikely [12] – in contrast to its behaviour in other dilute magnetic semiconductors such as GaAs:Mn [13] and ZnO:Mn [14]. However, the role of metallic clusters in determining the magnetic and electronic properties of transition metals in diamond has not been considered yet.

While models based on homogeneous distribution of magnetic dopants in a semiconducting host provide insight into DMS systems, it is important to also consider the effects of disorder and other configurations, including clustering of dopant atoms [5, 4]. We have previously [10] shown that substitutional Fe^{+1} in *p*-type diamond exhibits a half-metallic character, with a magnetic moment of $1.0 \mu_B$ per Fe ion and a large ferromagnetic stabilization energy of 33 meV. In this study, therefore, we investigate the properties of Fe^{+1} clusters in diamond using *ab initio* Density Functional Theory electronic structure methods. We consider the stability of different cluster configurations of Fe^{+1} and show that Fe ions have a strong tendency to form clusters in diamond, with the electronic structure of the most stable configuration being insulating. This is in contrast to the results of homogeneous distribution of Fe, where half metallic magnetic ordering is predicted. Further, we find that larger clusters suppress the induced magnetic moment, while being energetically more favourable compared to smaller clusters. These findings explain various previously perplexing experimental results in other dilute magnetic semiconductor such as the observed strong dependence of the magnetization on growth conditions such as temperature and annealing in Cu:ZnO [15], Cr:GaN [16] and Mn:GaAs [17].

2. Method

The properties of embedded Fe^{+1} clusters in diamond have been studied using *ab initio* Density Functional Theory calculations, as implemented in the CASTEP code [18]. The Perdew-Burke-Ernzerhof generalized gradient approximation [19], incorporating the on-site coulomb interaction parameter (GGA+*U*) was used to treat exchange-correlation effects, while Vanderbilt ultrasoft pseudopotentials [20] were used for valence-core interactions.

A well converged $4 \times 4 \times 4$ Monkhorst-Pack *k*-grid sampling [21] for integration over the Brillouin zone (32 *k*-points in the irreducible wedge of the Brillouin zone) was employed for spin and geometry optimization, with an optimized plane wave cut-off energy of 310 eV. Increasing the plane wave cut-off energy or number of *k*-points resulted in negligible changes in the energy, structural relaxation and magnetic effects (less than 10^{-4} eV, 10^{-3} Å, and $10^{-1} \mu_B$, respectively).

Geometry optimization, binding energy, and electronic structure calculations of the embedded Fe^{+1} clusters were carried out using a 64-atom diamond supercell constructed from $2 \times 2 \times 2$ conventional fcc diamond unit cells with an optimized lattice constant of 3.569 Å, in close agreement with the experimental value of 3.567 Å [22]. Various clusters sizes (Figure 1) consisting of up to four Fe atoms at substitutional sites in the diamond supercell were considered, and Full geometry optimization was performed without any symmetry or spin restrictions for each cluster in order to determine the most stable cluster configuration. Also, various initial spins from $0\mu_B$ to $6\mu_B$ were considered for each cluster configuration in order to determine the most stable spin states corresponding to the ground state geometries.

The binding energy E^b of each cluster complex configuration was determined by comparing its complex formation energy with that of its constituent defects relative to the limit in which the defects are well separated as [23, 24]

$$E_{A_x B_y}^b = E_{A_x B_y} + E_N - \{E_{A_x} + E_{B_y}\} \quad (1)$$

where $E_{A_x B_y}$ is the total energy of the cluster complex consisting of *x* atoms of defect A and *y* atoms of defect B, while E_N is the total Energy of pristine diamond, calculated in the same defect charge state, i.e. $q = +1$.

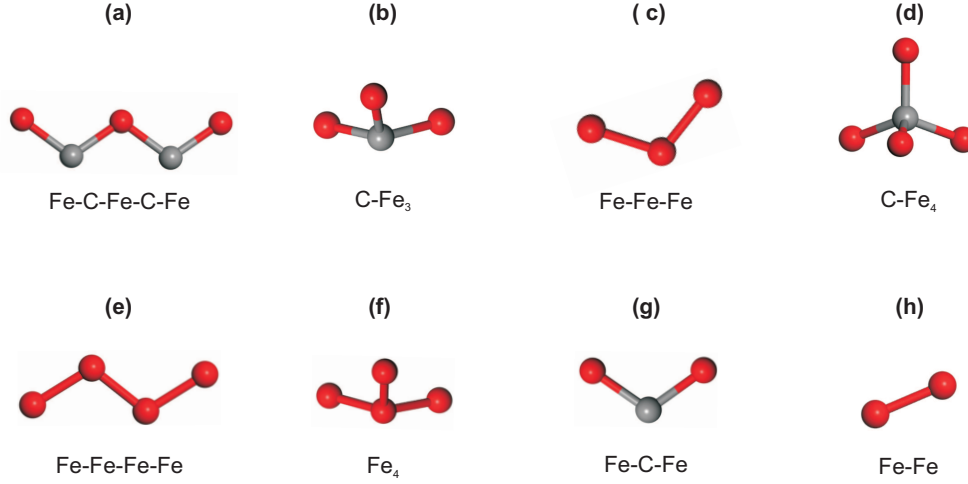


Figure 1. (Color online) Various possible cluster configurations of substitutional Fe⁺ in diamond (red balls represent Fe atoms, while grey balls represent C atom).

3. Results and discussion

Table 1. Binding energies of various Fe⁺ cluster configurations in diamond together with point symmetry and net induced spin per Fe⁺ ion.

Configuration	Structure (Figure 1)	Number of Fe ions	Symmetry	Net spin per Fe ⁺ ion (μ_B)	Binding energy (eV)
Fe-C-Fe-C-Fe (chain)	(a)	3	C_{2v}	0.5	-3.05
C-Fe-Fe-Fe (C-Fe ₃)	(b)	3	C_{3v}	0.9	-3.05
Fe-Fe-Fe (chain)	(c)	3	C_s	0.3	-2.07
C-Fe-Fe-Fe-Fe (C-Fe ₄)	(d)	4	C_{2v}	0.1	-1.84
Fe-Fe-Fe-Fe (chain)	(e)	4	C_s	0.0	-1.75
Fe-Fe-Fe-Fe (Fe ₄)	(f)	4	C_s	0.0	-1.75
Fe-C-Fe (chain)	(g)	2	C_{2v}	0.9	-1.84
Fe-Fe (chain)	(h)	2	C_{3v}	0.8	-0.49

Table 1 summarizes the calculated binding energies of the various Fe⁺ cluster configurations (Figure 1) as well as their point symmetries and net induced magnetic moments in diamond. We see that all the considered cluster configurations have negative binding energies, ranging from -3.05 eV to -0.49 eV, indicating that Fe ions have a strong tendency to form clusters in diamond, as opposed to a homogeneous spatial distribution. The magnitude of calculated binding energies is dependent on the cluster size and bonding of Fe ions within the cluster, with small clusters of two Fe ions being energetically unfavourable (by up to 2.6 eV) compared to those with three or four Fe ions. We find that clusters containing interspersed or alternating chains of Fe-C atoms are energetically most favorable. Also, the difference in binding energy between some cluster configurations is similar, suggesting that various cluster sizes consisting of different number of Fe atoms and arrangement can co-exist, particularly considering that dilute

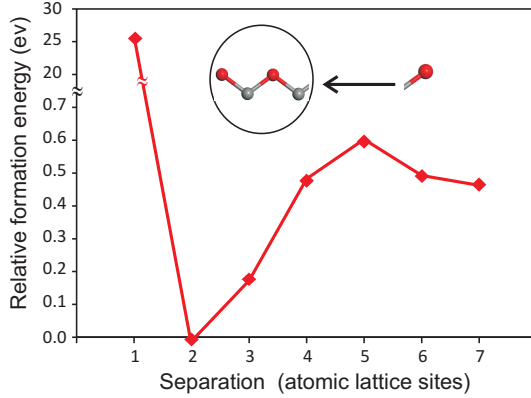


Figure 2. Formation energies of Fe-C-Fe ion cluster as a function of separation distance with a third Fe ion.

magnetic semiconductor systems are often grown under non-equilibrium conditions. Therefore, the statistical distribution, and consequently the electronic and magnetic properties of Fe-doped diamond, will depend sensitively on details of the growth conditions and other factors such as the mobility of dopants.

Importantly, the induced magnetic moment per Fe ion also depends sensitively on the cluster size and arrangement of Fe atoms, with larger cluster sizes ($n > 3$) suppressing the induced spin moments. Therefore, Fe is likely to form clusters in diamond during annealing while quenching the induced magnetic moment. This result is consistent with the experimentally observed decay in saturation magnetic moments upon annealing in some dilute magnetic semiconductors, such as Cu:ZnO [15], Cr:GaN [16] and Mn:GaAs [17]. This trend is expected based on increased dopant mobility during annealing, which in turn enhances formation of clusters, leading to suppressed magnetization.

In order to determine the nature of the embedded Fe clusters in diamond, we have also systematically studied the stability of the most stable cluster configuration (the Fe-C-Fe-C-Fe chain bonded cluster), with the third Fe ion at varying separations, using a large 128 atom supercell, as depicted in Figure 2. We see that the formation energy reaches a minimum when the third Fe atom is at the 2nd nearest neighbour separation, thus forming the stable Fe-C-Fe-C-Fe chain bonded cluster. As expected, moving the third Fe ion further to the nearest neighbour position causes a significant increase in formation energy (by 25 eV), due to electrostatic repulsive interactions. This indicates that alternating Fe-C clusters, with a C atom in between, are more stable compared to simple Fe-Fe bonded pair formation, consistent with the predictions of Mn:GaN [25], where the formation energies of directly bonded Mn-Mn cluster configurations are found to be energetically unfavourable.

3.1. Electronic properties and magnetic interactions

Figure 3 illustrates the density of states of the most stable embedded Fe cluster bonding configuration (Fe-C-Fe-C-Fe), as well as that of single substitutional Fe in diamond consisting of a uniform spatial dopant distribution. We find that clustering of Fe introduces multiple spin polarized impurity states in the diamond band gap, as opposed to single substitutional doping. We also find that hybridization between the carbon sp^3 orbitals and Fe $3d$ orbitals is stronger in the case of embedded Fe clusters as compared to single substitutional Fe. This strong orbital hybridization in the case of embedded cluster leads to band splitting and the formation of a deep localized Fe- $3d$ orbital, which may explain the origin of the observed clustering tendency.

Further, we find that while single substitutional Fe has an electronic structure with half metallic character and 100% spin polarization at the Fermi level, the aggregation of Fe and formation of embedded Fe clusters in diamond renders the system insulating. This observation helps to elucidate hitherto puzzling discrepancies between experimental data and theoretical predictions in other dilute magnetic semiconductors. For example, in Mn: GaN, theoretical investigations predict the system to be half metallic, whereas experimental results show that the system is highly resistive and insulating [26], is likely due to neglect of random distribution of dopants in the host semiconductor and clustering effects. Thus, these results highlight the importance of considering defect dynamics, distribution and aggregation to the understanding of the properties of transition metal dopants in diamond as well in other dilute magnetic semiconductors.

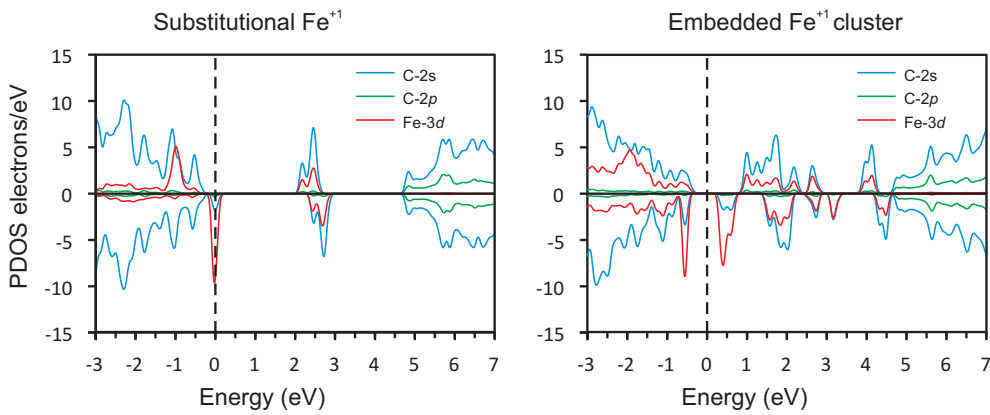


Figure 3. Partial Density of states of single substitutional Fe^{+1} and embedded Fe-C-Fe-C-Fe cluster in diamond.

4. Conclusion

We have systematically investigated the stability and spin interactions of embedded substitutional Fe^{+1} clusters in diamond using DFT+ U electronic structure methods. Our results show that Fe ions have a strong tendency to form clusters in diamond. We find that larger clusters (of more than three Fe ions) are more stable compared to smaller clusters, while suppressing the induced magnetic moments. Therefore, Fe is likely to form clusters in diamond during annealing while quenching the induced magnetic moment. We also find that, while the electronic structure of single substitutional Fe has a half metallic character with 100% spin polarization at the Fermi level, the aggregation of Fe and formation of embedded Fe clusters in diamond renders the system insulating.

These results may explain the experimentally observed decay in saturation magnetic moments after annealing in some dilute magnetic semiconductors [15, 16, 17], which can be understood based on increased dopant mobility during annealing, which in turn enhances formation of clusters, leading to suppressed magnetization. Further, our results shed light on previous discrepancies between experimental data and theoretical predictions in other dilute magnetic semiconductors, for example, in Mn: GaN [26] where theoretical investigations predict the system to be half metallic, whereas experimental results show that the system is highly resistive and insulating. These results highlight the importance of considering the effect of distribution and aggregation of dopants to the understanding of the properties of transition metal dopants in dilute magnetic semiconductors.

- [2] Ohno H 1998 *Science* **281** 951
- [3] Wolf S A , Awschalom D D, R. A. Buhrman R A, Daughton J M, von Molnar S, Roukes M L, Chtchelkanova A Y and Treger D M 2001 *Science* **294** 1488
- [4] Dietl T 2010 *Nature Mater.* **9** 965
- [5] Chambers S 2010 *Nature Mater.* **9** 956
- [6] Sussmann R S 2009 *CVD Diamond for Electronic Devices and Sensors* (John Wiley and Sons Ltd., United Kingdom)
- [7] Balasubramanian G, Neumann P, Twitchen D, Markham M, Kolesov R, Mizuochi N, Isoya J, Achard J, Beck J, Tissler J, Jacques V, Hemmer P R, Jelezko F and Wrachtrup J 2009 *Nature Mater.* **8** 383
- [8] Dietl T, Ohno H and Matsukura F 2001 *Phys. Rev. B* **63** 195205
- [9] Greentree A D, Fairchild B A, Hossain F M and Prawer S 2008 *Mater. Today* **11** 22
- [10] Benecha E M and Lombardi E B 2013 *J. Appl. Phys.* **114** 223703
- [11] Benecha E M and Lombardi E B 2011 *Phys. Rev. B* **84** 235201
- [12] Erwin S C and Hellberg C S 2003 *Phys. Rev. B* **68** 245206
- [13] Macdonald A H, Schiffer P and Samartha N 2005 *Nature Mater.* **4**, 195
- [14] Sharma P, Gupta A, Rao K V, Owens F J, Sharma R, Ahuja R, Guillen J M O, Johansson B and Gehring G A 2003 *Nature Mater.* **2** 673
- [15] Buchholz D B, Changa R P H, Song J H and Ketterson J B 2005 *Appl. Phys. Lett.* **87** 082504
- [16] Singh R K, Wu S Y, Liu H X, Gu L, Smith D J and Newman N 2005 *J. Appl. Phys.* **86** 012504
- [17] Moreno M, Trampert A, Jenichen B, Dweritz V and Ploog K H 2002 *J. Appl. Phys.* **105** 073911
- [18] Clark S J, Segall M D, Pickard C J, Hasnip P J, Probert M J, Refson K and Payne M C 2005 *Z. Kristallogr.* **220** 567
- [19] Perdew J P, Burke K and Ernzerhof M 1996 *Phys. Rev. Lett.* **77** 3865
- [20] Vanderbilt D 1990 *Phys. Rev. B* **41** 7892
- [21] Monkhorst H J and Pack J D 1976 *Phys. Rev. B* **13** 5188
- [22] Donnay J D H and Ondik H M 1973 *Crystal Data: Determinative Tables* 3rd ed. (U.S. Department of Commerce National Bureau of Standards JCPDS) Vol. 2.
- [23] Raebiger R, Nakayama H and Fujita T 2014 *J. Appl. Phys.* **115** 012008
- [24] Mahadevan P, Osorio-Guillen J M and Zunger A 2005 *Appl. Phys. Lett.* **86** 172504
- [25] Cui X Y, Delley B, Freeman A J and Stampfl C 2007 *Phys. Rev. B* **76** 045201
- [26] Dhar S, Brandt O, Trampert A, Friedland K J, Sun Y J, and Ploog K H 2003 *Phys. Rev. B* **67** 165205; Dhar S, Brandt O, Trampert A, Daweritz L, Friedland K J, Ploog K H, Keller J, Beschoten B and Guntherodt G 2003 *Appl. Phys. Lett.* **82** 2077